Hindawi
Advances in Civil Engineering
Volume 2018, Article ID 7891914, 12 pages
https://doi.org/10.1155/2018/7891914

Research Article

The Mass Loss Behavior of Fractured Rock in Seepage Process: The Development and Application of a New Seepage Experimental System

Hailing Kong[1,2] **and Luzhen Wang**[1,2]

[1]*Civil Engineering Department, Yancheng Institute of Technology, Yancheng, Jiangsu 224051, China*
[2]*School of Civil, Environmental & Mining Engineering, The University of Adelaide, Adelaide, SA 5005, Australia*

Correspondence should be addressed to Luzhen Wang; wangluzhen5@126.com

Received 5 June 2018; Accepted 14 August 2018; Published 18 October 2018

Academic Editor: Yan Peng

In order to study the water-inrush mechanism in fractured geological structure, seepage instability theory is picked up, which considers that water-inrush is the embodiment of seepage instability. Seepage tests are the basis for studying seepage instability in the fractured rock system, while the experimental system and equipment are the foundation of seepage tests. In this paper, we introduce a new experimental system for the seepage test on fractured rock accompanying with mass migration and loss and discuss its development and application. It presents the designed and manufactured experimental system, the subsystems, components and their functions, and the experimental scheme and the experimental process. Compared to the previous experimental system, more functions are satisfied, among which, the most important improvements are realizing a long-term permeate and keeping water pressure stable at a high level. These improvements are verified by a series of tests, and the results show that our experimental system has higher accuracy, stability, and reliability. The distribution of the permeate times and lost mass of different Talbol power exponents are obtained, and the time-varying rules of water pressure, water flow, the lost mass, and porosity are also revealed through the results. Although the experimental system also has some limitations, for instance, the measuring accuracy of pressure transducers and flow transducers, the provided maximum pressure of the quantitative displacement piston pump, the fine particles collection subsystem, etc., we will continue to improve it in our further research.

1. Introduction

Due to the increasing demand for coal resources and gradual exhaustion of the shallow resources, deep excavation is more and more common in most coal mines in China. However, deep coal seams usually have very complex geological structure [1], for instance, fractures, faults, collapse column, and so on. Excavation in deep mines is often accompanied with water-inrush accidents, which bring serious threats to the safe production of coal mines [2, 3].

Water-inrush mechanism becomes one of the hottest research points in academia. Some scholars consider that fractures develop and expand in the surrounding rock under mining and then connect with the fractured geological structure, resulting in water-inrush accidents, while some other scholars take the fractured geological structure itself as a water-inrush channel and consider that water-inrush happens directly if water pressure is satisfied. Former studies often focused on the mining effect on water-inrush in the fractured geological structure [4–11]; on the contrary, latter studies preferred to pay more attention to the permeate properties of the fractured rock.

The research team in China University of Mining and Technology had carried out a series of related theoretical and experimental research studies on the permeability of fractured rock based on the MTS 815 rock mechanics servo-controlled testing system [12–23]. They considered that water flow in the fractured rock disobeyed Darcy's law, seemed the seepage

system of fractured rock as a nonlinear dynamic system, and analyzed the stability and bifurcation of the system by Lyapunov's first method to reveal water-inrush mechanism in coal mines with fractured geological structure [12, 13], which is named "seepage instability theory".

Whether the condition of seepage instability can be realized physically is the key point of seepage instability theory to explain water-inrush; in other words, only the non-Darcy flow β factor is negative, seepage instability will happen, and water-inrush occurs. The sign of the non-Darcy β factor [24–26] is based on the MTS815 rock mechanics servo system. When the phenomenon of mass migration and loss was observed in seepage tests, scholars began to study whether the sign of the non-Darcy β factor has any relevance to this phenomenon. But restricted by the supercharger volume in the permeate circuit in the MTS testing system, they could not study further anymore.

To overcome the defect of the small supercharger volume in the permeate circuit, Yao [27] designed an equipment, tested the fluid flow change rule under the conditions of different proportion, axial pressure, and so on, but the equipment could only test the fluid flow change for 3 minutes, which is the greatest shortage of this equipment. Then it was improved, shortening the piston and lengthening the overflow tank [28]. Unfortunately, there is still a defect that the precision of pressure control is not high enough. Subsequently, a permeate circuit and a test system were designed for testing the permeability of fractured rock, which adapted to the requirement of longer time penetration, and the inlet pressure of the rock specimen must remain stable [29]. To realize a long-term permeate under a stable pressure, a sustainable pressurized osmosis device for the seepage test of rock mass which could control pressure stability for a long time was designed and patented [30].

Even though these research studies consider mass migration and loss in the fractured rock during the permeate process, they failed to realize the free migration of the particle in a long-term seepage test.

In this paper, a new seepage testing system is introduced, realizing a long-term permeate under the stable pressure and free migration of the particle in fractured rocks, which is used to test permeate properties of fractured rock accompanying with mass migration and loss to study the catastrophe rule of permeate in fractured rocks, which will provide research reference for judging seepage instability or even reveling water-inrush mechanism in coal mines with fracture geological structure.

2. Materials and Methods

2.1. The Experimental System

2.1.1. The Functional Requirements of the Experimental System. In order to satisfy the demand for seepage tests on fractured rock accompanying with mass migration and loss, kinds of factors are taken together, and the functional requirements of the experimental system are summarized, including axial loading and displacement controlling, long-term permeating, sealing, pressure controlling, water-flow direction controlling, data collecting, filtrating and dehydrating, cooling, permeation modes switching, opening, and loss particle collecting.

Particularly, some functions are realized for the first time by our experimental system for the seepage test on fractured rock accompanying with mass migration and loss.

For instance, the experimental system should have the function of long-term permeating and pressure controlling, so that, during the test process, our experimental system can deliver water to the specimen uninterruptedly for a long time with a stable constant pressure or constant flow rate, maintain a stable pressure difference between the two ends of specimens for a long time, adjust the pressure of the entrance end of the specimen to study the non-Darcy flow permeate properties, as well as realize a long-term permeating, that is, make water flow into one end of the specimen freely and flow out of the other end.

Our experimental system also can switch between the two permeation modes: the syringe penetration method or the pump station penetration method, which solves the problems in traditional equipment and systems, for example, the previous systems could not control and adjust water pressure; besides, they could not provide water with stable pressure for seepage tests. Now, our experimental system can provide water continuously with a stable and controllable water pressure as we introduce the switching between the syringe penetration method and the pump station penetration method [31].

The two functions above and the other satisfied functions will improve the accuracy of the seepage tests for fractured rock.

2.1.2. The Design of the Experimental System. The designed experimental system for the seepage test on fractured rock accompanying with mass migration and loss is shown in Figure 1, consisting of four subsystems, the axial-loading and displacement-controlling subsystem, the fluid flow subsystem, the fine-particles collection subsystem, and the data acquisition-analysis subsystem.

(1) The Axial-Loading and Displacement-Controlling Subsystem. The axial-loading and displacement-controlling subsystem contains a 30-ton hydraulic material-testing machine to satisfy the demand for stiffness, a variable displacement piston pump to support power, a reversing valve and a relief valve to change the power, a single-action hydraulic cylinder to load and change the axial displacement of the specimen, and a displacement transducer to control the displacement of the specimen.

When testing, the single-action hydraulic cylinder is set on the loading platform of the material-testing machine, power is given and controlled by the variable displacement piston pump, the reversing valve and the relief valve, which can control the loading speed of the single-action hydraulic cylinder, to change the axial displacement of the specimen accurately, and the displacement of the specimen is required by the displacement transducer.

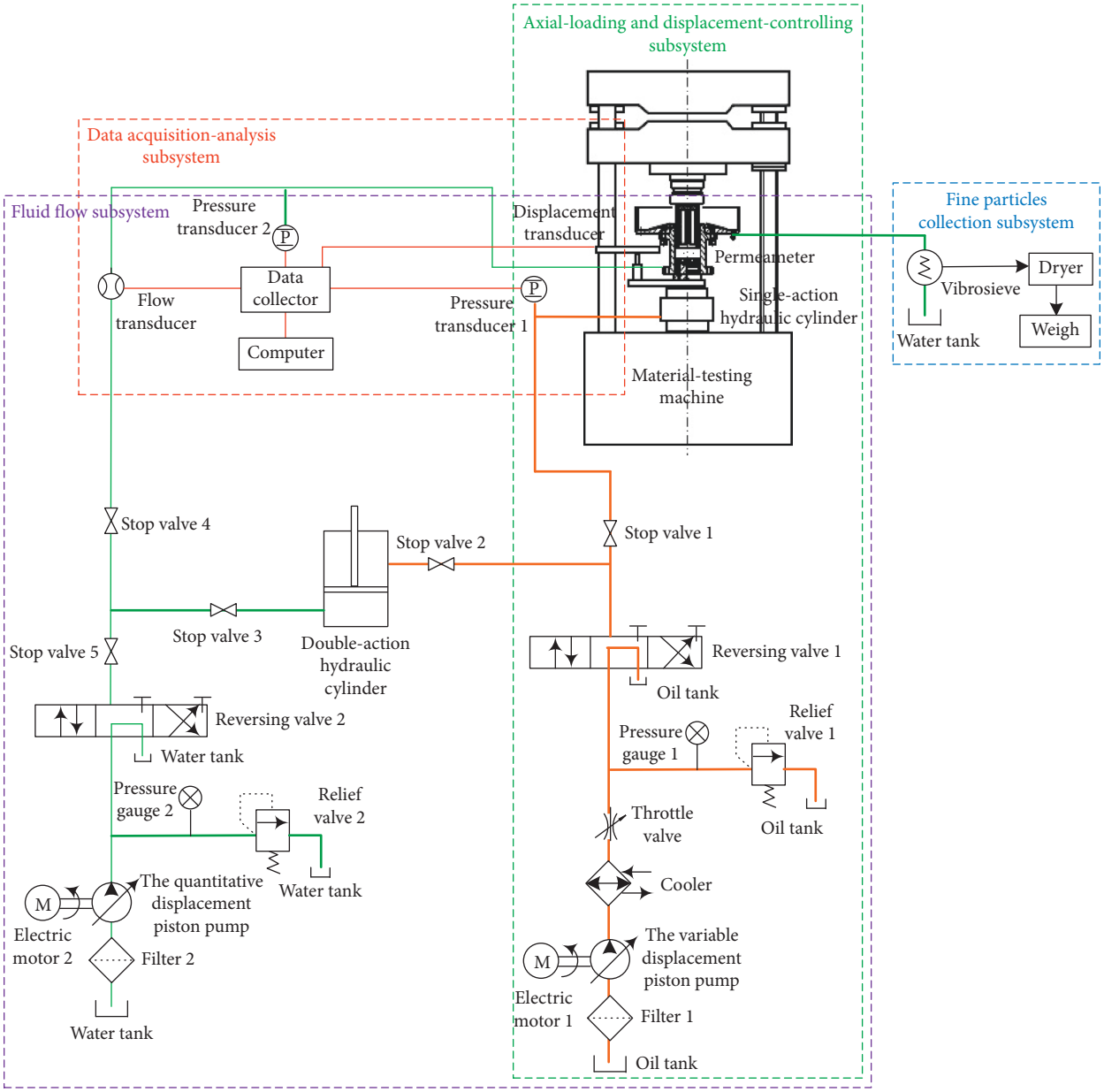

Figure 1: The design of the experimental system.

(2) The Fluid Flow Subsystem. The fluid flow subsystem contains a permeameter to fill the specimen, a variable displacement piston pump and a quantitative displacement piston pump to provide power to drive the water flow, reversing valves and relief valves to change the power, a double-action hydraulic cylinder to realize a reality water seepage test by driving water flow by oil pressure, and a pressure transducer and a flow transducer to gather data.

The fluid flow subsystem includes two kinds of permeation circuit, a syringe permeation circuit and a pump permeation circuit, and the two can switch to each other.

The syringe permeation circuit contains the variable displacement piston pump, reversing valves, relief valves, the double-action hydraulic cylinder, etc. When testing, we first adjust the reversing valve 1, open stop valves 2, 3 and 5, close stop valves 1 and 4, inject water into the inferior vena cava in the double-action hydraulic cylinder by the quantitative displacement piston pump, and close stop valve 5 after injection; secondly, adjust the reversing valve 1, open stop valve 4, inject hydraulic oil into the superior vena cava in the double-action hydraulic cylinder through the cooler, throttle valve, and reversing valve 1, and stop valve 2 by the variable displacement piston pump to push the piston rod into the double-action hydraulic cylinder downward using hydraulic oil; thirdly, drive water in the inferior vena cava into the permeameter through stop valves 3 and 4 and the flow transducer, control the oil pressure in the superior vena cava by relief valve 1, and control the pore pressure in the lower end of fractured rock specimens indirectly; and lastly, record the data of the pore pressure and the inrushing water flow by

using the pressure transducer and flow transducer in real time during the fluid flow process.

The pump permeation circuit contains the quantitative displacement piston pump, relief valves, etc. When testing, we first open stop valves 4 and 5, close stop valve 3, adjust the reversing valve 2; secondly, drive water into the permeameter through the reversing valve 2, stop valves 4 and 5, and the flow transducer by the quantitative displacement piston pump; and lastly, record the data of the pore pressure and the inrushing water flow by using the pressure transducer and flow transducer in real time during the fluid flow process.

(3) The Fine Particles Collection Subsystem. The fine particles collection subsystem contains a vibrosieve, a filter screen, a dryer, etc. When testing, we collect fine particles by using the vibrosieve and filter screen after the fine particles migrate with water flow out of the permeameter and then dry them and weigh them.

(4) The Data Acquisition-Analysis Subsystem. The data acquisition-analysis subsystem consists of a data collector, a computer, and transducers in the other three subsystems. When testing, the physical parameters, such as pressure and water flow, are acquired by transducers, collected by the data collector, and recorded by the computer.

2.1.3. The Real Manufactured Experimental System. The real manufactured experimental system is presented in Figure 2, which consists of the four subsystems mentioned above.

The important parts of the axial-loading and displacement-controlling subsystem are shown in Figure 3, the left of which is the single-action hydraulic cylinder, whose maximum traverse is 50 mm, and the right one is the variable displacement piston pump, the model of which is SCY14-1B; its rated pressure is 31.5 MPa, and its permissions error is ±4%.

The permeameter is the most important component of the fluid flow subsystem. The details of the permeameter, such as floor, cylinder, permeable plate, piston, overflow tank, and the lost fine particles-collecting tank, are presented in Figure 4.

Water intakes and two sealing grooves are fixed and milled on the floor. The inner diameter of the cylinder is 100 mm. Grooves and holes are distributed on the permeable plate, which will make the equidistribution of water pressure when water flows into the cylinder. The piston is with a height of 25 mm, and 19 holes with the diameter of 10 mm are manufactured on the piston, looking like a honeycomb briquette. Six large exits with the height of 115 mm are around the cylinder of the overflow tank. The unique design of piston and overflow tank makes sure that the fine particles can migrate freely, which is the key component of the permeameter to realize permeate in fractured rock accompanying with mass migration and loss. The lost fine particles-collecting tank has an outlet to make sure the crushed-out fine particles flow with water through the pipe to the fine particles collection subsystem.

Figure 2: The experimental system.

The other parts of the fluid flow subsystem include the quantitative displacement piston pump and the double-action hydraulic cylinder, which are shown in Figures 5(a) and 5(b). The quantitative displacement piston pump can provide a maximum pressure of about 8 MPa, and its work pressure is 7 MPa, and maximum displacement is about 600 L per hour. The double-action hydraulic cylinder with an inner diameter of 220 mm has a piston with a diameter of 160 mm, and its maximum traverse and volume are 500 mm and 20 L, respectively.

The vibrosieve and filter screen in the fine particles collection subsystem are shown in Figure 6. The model of vibrosieve is 450, and the filter screen is the 300-mesh fine gauze, and the corresponding collected grains size could reach 48 microns.

The main components of the data acquisition-analysis subsystem, for instance, data collector, pressure transducer, flow transducer, and pressure gauge are shown in Figure 7. The data collector is the model of HWP2100R, which works with the matching data-collection software Dolgger, improving the processing and analysis speed of test data greatly. The model of the pressure transducer is BP800, whose measure traverse and measure accuracy are 16 MPa and 2 kPa, respectively. The flow transducer is a LZ series metal tube flow transducer with high accuracy, stability, and reliability.

2.1.4. Supplementary Instructions. The four subsystems mentioned above are seemed relatively independent, but it is for their structures, not functions. Sometimes, a function of this experimental system can be afforded by two or even three subsystems. For example, as mentioned in the functional requirements of the experimental system, the experimental system should have the function of collecting data of pressure and the amount of water flow real timely, automatically and efficiently, but this function is afforded by the whole experimental system except for the axial-loading and displacement-controlling subsystem. Besides, one subsystem also can afford several functions. Taking the fluid flow subsystem as the example, it affords the functions of seal, openness, and collecting loss particle.

There are three quantitative displacement piston pumps in the permeation circuit, which can work alternatively to avoid high temperature of the pump and realize a long-time continuous penetration test.

(a) (b)

Figure 3: The (a) single-action hydraulic cylinder and (b) variable displacement piston pump.

(a) (b) (c)

(d) (e) (f)

Figure 4: Permeameter. (a) Floor, (b) cylinder, (c) permeable plate, (d) piston, (e) overflow tank, and (f) lost fine particles-collecting tank.

2.2. The Seepage Experiments. In order to verify that whether our experimental system has satisfied all the functions mentioned above, we carry out a series of seepage tests on fractured rock accompanying with mass migration and loss.

2.2.1. The Experimental Scheme. We use the Talbol continuous grading formula [32] to match the specimen, and the power exponents n are 0.1, 0.2, ..., 0.9 and 1.0. These specimens are charged and compacted to 120 mm, 123 mm,

(a) (b)

Figure 5: The (a) quantitative displacement piston pump and (b) double-action hydraulic cylinder.

(a) (b)

Figure 6: The (a) vibrosieve and (b) filter screen.

and 126 mm, and the loaded water pressure on the bottom of the specimen are 3 MPa, 5 MPa, and 7 MPa, respectively.

When designing the experimental scheme, several functions should be considered, such as long-term permeate, controlling pressure to keep water pressure stable, and the switch between the syringe penetration method and the pump station penetration method. Therefore, the experimental scheme is listed as in Table 1.

2.2.2. The Experimental Process. The experimental process of the seepage test on fractured rock accompanying with mass migration and loss is divided into several steps, as shown in Figure 8.

Experimental system installation and debugging will be going before testing, to ensure that the seepage tests could carry out successfully. We must make sure that the water pressure researches 8 MPa, observe whether there is any leakage in the permeation circuit, check the data collector and transducers, etc, and we should test the system operation.

Mixing and charging ingredients also will be done before testing. We mix kinds of particles with different sizes after weighing based on the mixture ratio, charge the mixture into the permeameter and compact the specimen, and then calculate the natural porosity of the specimen.

As the permeameter is assembled into the experimental system, the specimen is initially loaded to 0.02 MPa and then loaded to the set displacement, and the initial porosity of the specimen is calculated. Subsequently, injecting water into the specimen for half an hour until the specimen is saturated.

When the seepage tests start, we open the quantitative displacement piston pump and inject water into the double-action hydraulic cylinder.

After adjusting water pressure to the set value, water starts to permeate through the specimen till seepage instability, water pressure, and flow are acquired and recorded

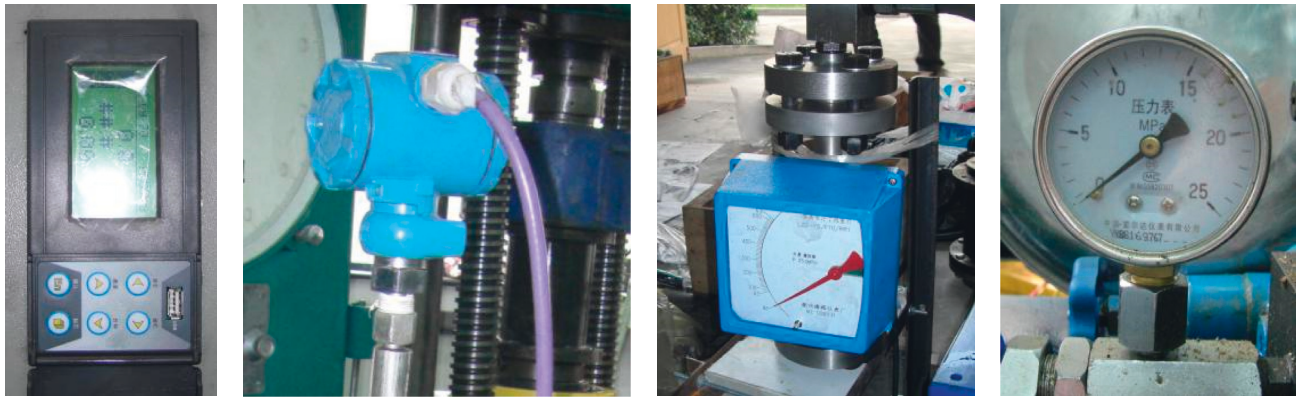

(a) (b) (c) (d)

Figure 7: The main components of the data acquisition-analysis subsystem. (a) Data collector, (b) pressure transducer, (c) flow transducer, and (d) pressure gauge.

Table 1: The experimental scheme.

		The loaded water pressure		
		3 MPa	5 MPa	7 MPa
The initial height	120 mm	$n = 0.1, 0.2, \ldots, 0.9, 1.0$ each kind 3 times	$n = 0.1, 0.2, \ldots, 0.9, 1.0$ each kind 3 times	$n = 0.1, 0.2, \ldots, 0.9, 1.0$ each kind 3 times
	123 mm	$n = 0.1, 0.2, \ldots, 0.9, 1.0$ each kind 3 times	$n = 0.1, 0.2, \ldots, 0.9, 1.0$ each kind 3 times	$n = 0.1, 0.2, \ldots, 0.9, 1.0$ each kind 3 times
	126 mm	$n = 0.1, 0.2, \ldots, 0.9, 1.0$ each kind 3 times	$n = 0.1, 0.2, \ldots, 0.9, 1.0$ each kind 3 times	$n = 0.1, 0.2, \ldots, 0.9, 1.0$ each kind 3 times

real-timely. If seepage instability does not occur, restart the quantitative displacement piston pump, and repeat the seepage experiment.

The lost fine particles are collected at regular intervals till seepage instability; then the collected fine particles are numbered, dried, and weighed. At the end of the tests, the left specimen is discharged and then dried and weighed.

As the tests are finished, data are summarized and analyzed to reveal the rules of mass migration and loss in fractured rock during its permeate process.

3. Results and Analysis

3.1. The Achieved Long-Term Permeate in the Seepage Experiment. As we know, water-inrush results from seepage system instability of fractured rock based on the seepage instability theory, the permeate lasts a long time in the seepage system of the fractured rock till water flow changes which cause a water-inrush accident. It is necessary to study the long-term permeate in fractured rocks.

Taking the specimens with the initial height of 120 mm as examples, the distribution of permeate times of different Talbol power exponents under different water pressures is shown in Figure 9. As seen, the specimens with the Talbol power exponents of 0.3, 0.4, 0.5, and 0.6 always have a longer stable permeate process, when water pressure is 3 MPa, the stable permeate lasts at least 4000 s, and it lasts at least 600 s while the water pressure is 5 MPa; thus the original seepage system cannot afford such a long-term seepage test. The longest stable permeate lasts for about 18000 s when water pressure is 3 MPa, which is about 60 times of Yao's seepage system, whose permeate time is about 300 s [27].

3.2. The Stable Water Pressure and Water Flow. The time-varying curves of water pressure and water flow of the specimen are shown in Figure 10, the specimen's Talbol power exponent, initial height, and loaded water pressure are 0.5, 120 mm, and 3 MPa, respectively. Water flow remains nearly stable till water flow changes at about 18000 s, and water pressure also remains stable even though it has a small range of fluctuation, within the scope of the permissions error, satisfying our design function.

The most important improvements of the new seepage system completely satisfy our initial demands for the experimental system.

3.3. The Tested Permeability Parameters Characteristics in Time. Based on the collected time series of flow seepage and the pressure gradient, the permeability parameters, including permeability, non-Darcy flow β factor, and acceleration coefficient, can be calculated [33]. The time-varying rules of permeability parameters are obtained; we also take the samples with the Talbol power exponent of 0.5 as examples to display the time-varying rules of the permeability, the non-Darcy flow β factor, and the acceleration coefficient, as shown in Figure 11. In these experiments, permeability parameters are successfully obtained by the collected time

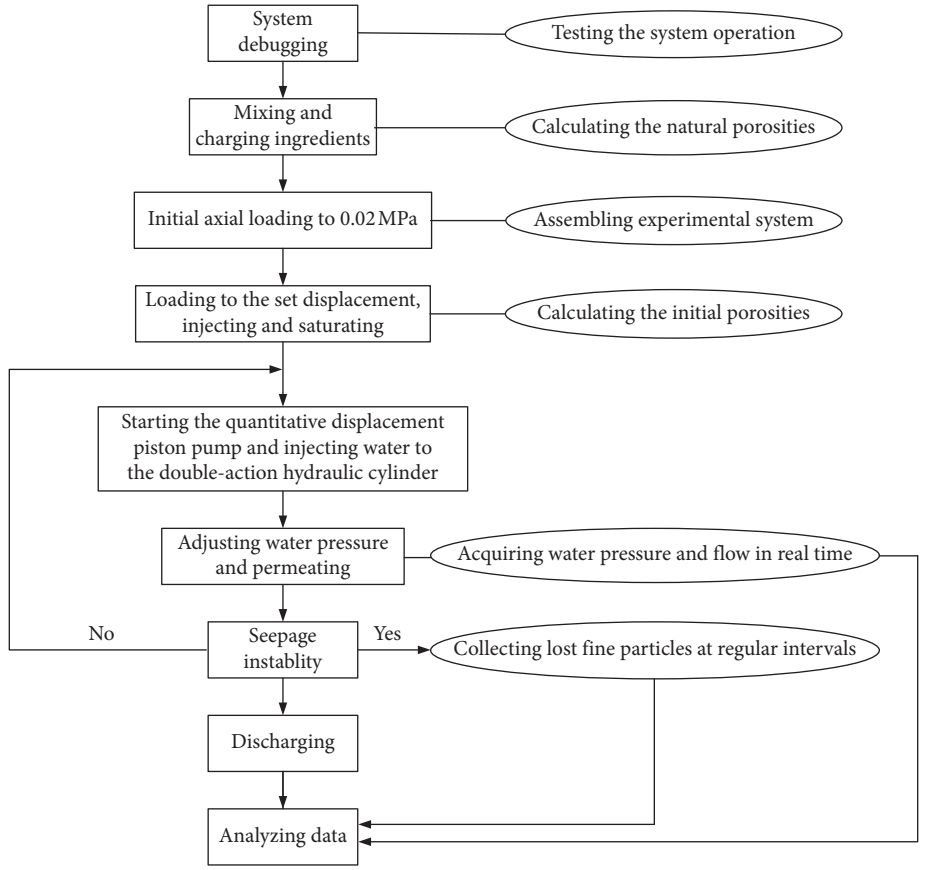

Figure 8: The experimental process.

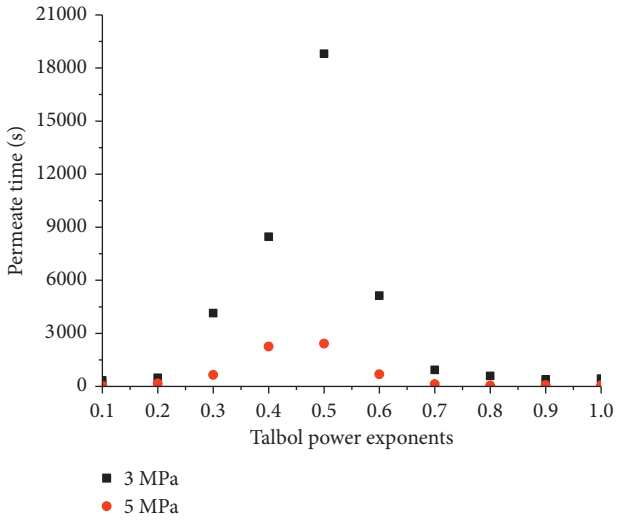

Figure 9: The distribution of permeate times of different Talbol power exponents.

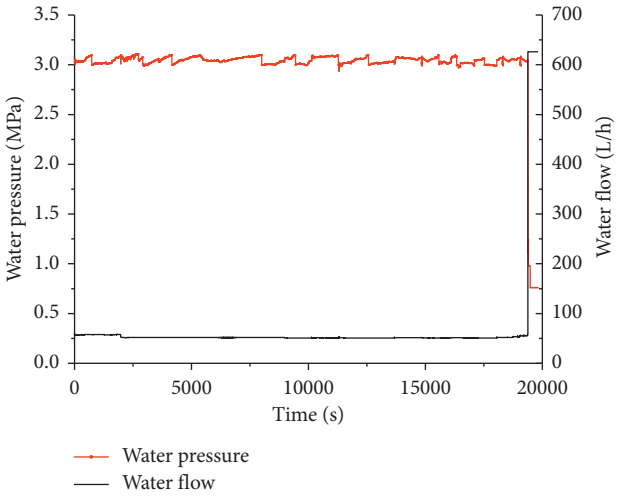

Figure 10: The time-varying curves of water pressure and water flow.

series of flow seepage and the pressure gradient, and the mutation characteristics of the permeability parameters are presented in the curves, as shown as the steps of these curves at the initial seepage stage.

3.4. The Mass Loss Behavior in the Fractured Rock during the Seepage Process. Also taking the specimens with the initial height of 120 mm and loaded water pressure of 3 MPa as examples, the permeate time and lost mass are shown in Figure 12.

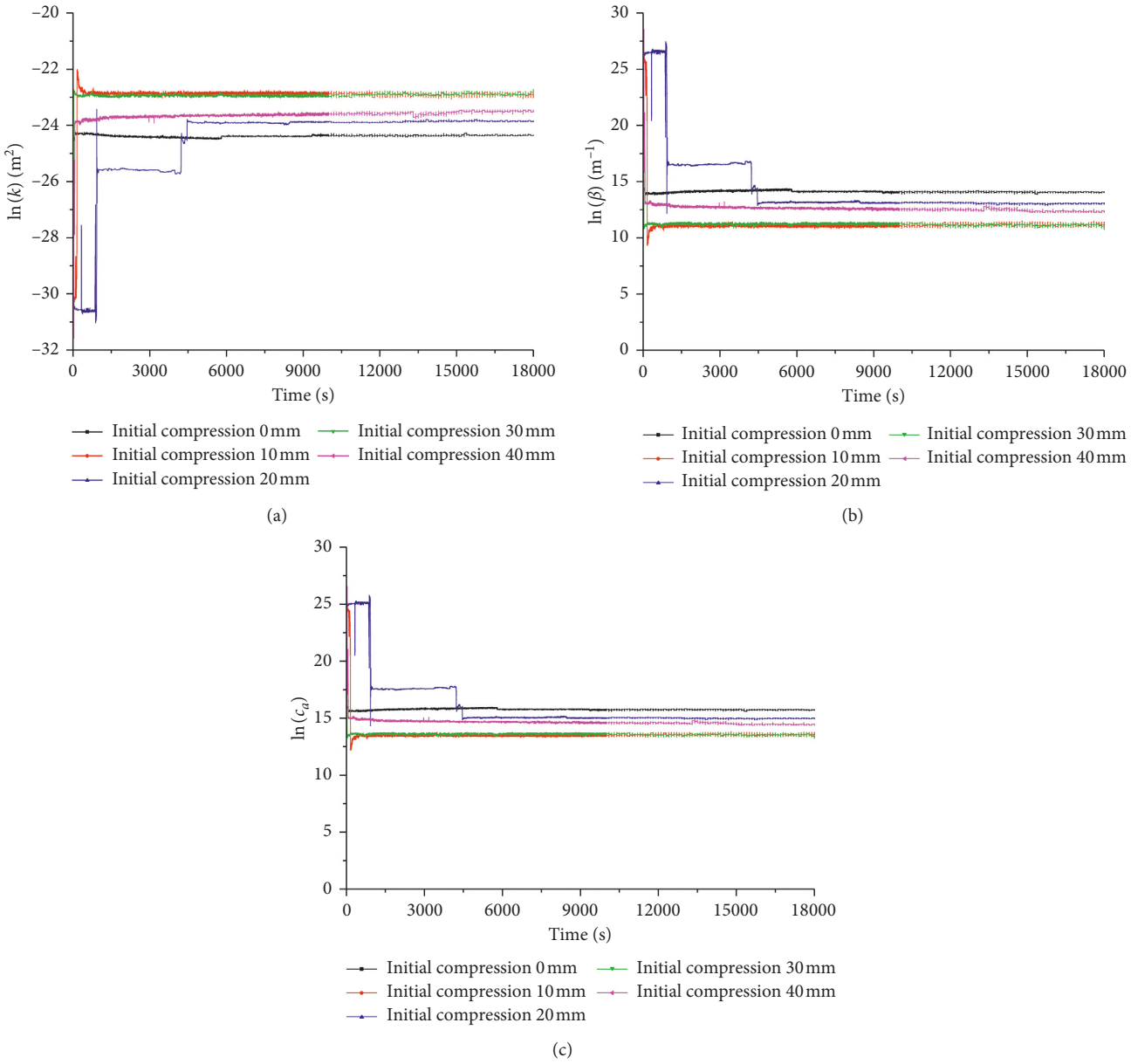

Figure 11: The permeability parameters characteristics in time. (a) Permeability, (b) non-Darcy flow β factor, and (c) acceleration coefficient.

As can be seen, specimens with smaller Talbol power exponents, such as 0.1, 0.2, and 0.3, have larger lost mass but have shorter stable permeate time because these specimens have higher proportions of fine particles, which can migrate and rush out of the specimens with water flow easily and quickly, so that the stable permeate time is very short; it is worth noting that the lost mass increases as the Talbol power exponent increases because specimens of larger power exponents have higher proportions of particles in larger size, which produce new fine particles under the compression and abrasion during the test process, and these newly produced fine particles also migrate and crush out.

For specimens with Talbol power exponents of 0.7, 0.8, 0.9, and 1.0, they have less lost mass and shorter stable permeate time, because of the higher proportions of particles in larger sizes, and their irregular arrangements, resulting in less lost mass and larger porosity; if the fine particles migrate from their structures, water flow channels are formed naturally, and as a result, they also have shorter stable permeate time.

Compared to specimens with Talbol power exponents of 0.1 to 0.3 and 0.7 to 1.0, specimens with Talbol power exponents of 0.4, 0.5, and 0.6 have lower proportions of fine particles and large size particles. During the test process, fine particles migrate with water flow, and new particles are produced under the compression and abrasion of those large size particles; the newly produced fine particles also migrate with water flow, but other particles block the pore partly in

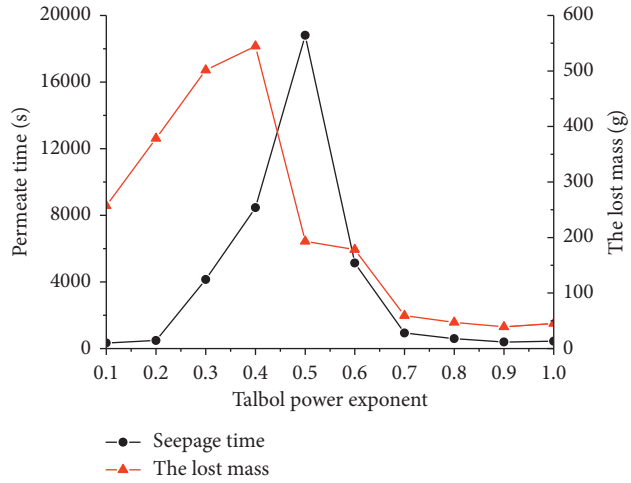

Figure 12: The permeate times and lost mass of different Talbol power exponents.

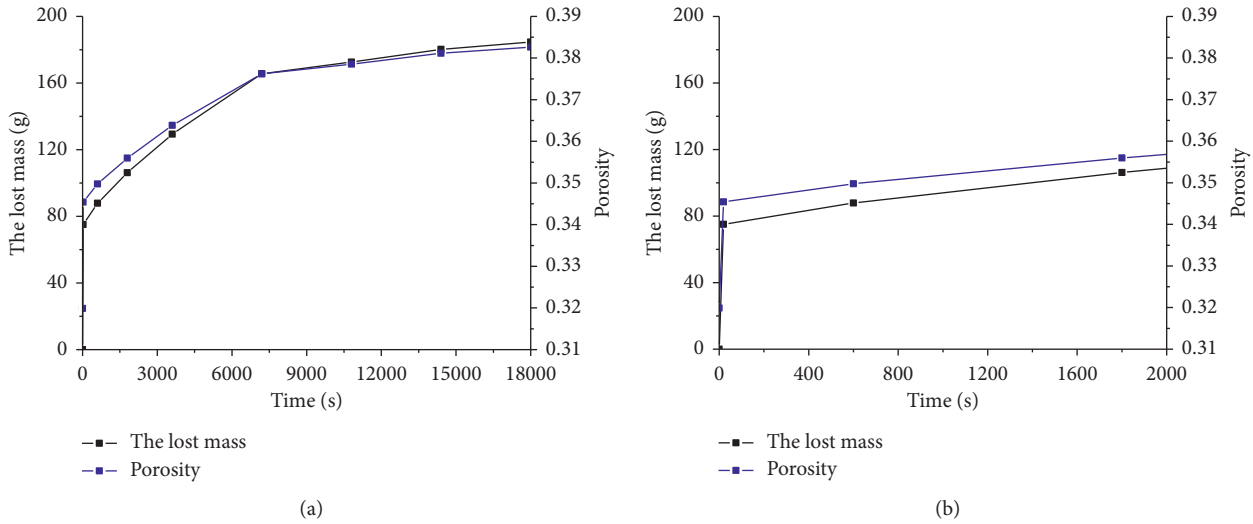

Figure 13: The time-varying rules of the lost mass and porosity.

the specimens even though fine particles are produced continuously, and they also migrate with water flow, but as the pore is blocked partly, fine particles cannot crush out of the specimens as easy as before, which result in the drop of the lost mass. The original fine particles migrate, and new particles are produced and supplied continuously; the structures of the specimens remain stable, so they have longer stable permeate time.

Taking the specimen with the Talbol power exponent of 0.5, initial height of 120 mm, and loaded water pressure of 3 MPa as an example, the time-varying rules of the lost mass and porosity [34] are shown as Figure 13, especially the time-varying rules in the first 2000 s, which is shown in the right figure. As Figure 13 shows, the lost mass increases with the increase in permeate time, and the varying curve of porosity is nearly the same as the lost mass. Obviously, the time-varying curve is divided into three stages; in the initial stage, the lost mass increases rapidly; in the middle stage, the lost mass decreases gradually and the increasing speed becomes slower and slower; and in the last stage, the lost mass nearly remains stable.

4. Conclusions and Expectations

Based on the seepage instability theory, water-inrush is the embodiment of seepage instability in fractured geological structure, and seepage tests are the basis of studying seepage instability of the seepage system in fractured rock, and experimental system and equipment are the basis of seepage tests. Combining the functional requirements, a new experimental system for the seepage test on fractured rock accompanying with mass migration and loss is designed and manufactured to overcome the defects in previous research studies and the experimental systems. The functions of subsystems and components are introduced, and the most important improvements of the new seepage system are realizing a long-term permeate and keeping water pressure stable on a high level, which are verified. The specimens are

taken as examples to show the distribution of the permeate times and lost mass of different Talbol power exponents and to revel the time-varying rules of water pressure, water flow, the lost mass, and porosity. What we obtain by our experimental system expresses a longer-time permeate process and higher accuracy, stability, and reliability.

The newly designed experimental system could be used in other fields if it is combined with other equipment, for example, if we use a glassy translucent material to manufacture the permeameter cylinder, problems in the permeate process can be researched combining CT equipment, such as the movement of fine particles and the damage of the fractured rock. Of course, there are still some aspects that need to be improved, for example, the measuring accuracy of pressure transducers and flow transducers; the provided maximum pressure of the quantitative displacement piston pump; and the fine particles collection subsystem, which are operated manually now. These shortages are what we devote to in the next stage.

Data Availability

The data used to support the findings of this study are available from the corresponding author upon request.

Conflicts of Interest

The authors declare that there are no conflicts of interest regarding the publication of this paper.

Acknowledgments

This work was supported by the Natural Science Foundation of Jiangsu Province of China (BK20160433 and BK20170477), the National Natural Science Fund (11502229), the Joint Open Fund of Jiangsu Collaborative Innovation Center for Ecological Building Material and Environmental Protection Equipments and Key Laboratory for Advanced Technology in Environmental Protection of Jiangsu Province, the Outstanding Young Backbone Teacher of QingLan Project in Jiangsu Province, Jiangsu Government Scholarship for Overseas Studies, Scholarship for Overseas Studies in Yancheng Institute of Technology, and the Program of Outstanding Young Scholars in Yancheng Institute of Technology.

References

[1] H. P. Xie, F. Gao, and Y. Ju, "Research and development of rock mechanics in deep ground engineering," *Chinese Journal of Rock Mechanics and Engineering*, vol. 34, no. 11, pp. 2161–2178, 2015.

[2] M. C. He, H. P. Xie, S. P. Peng, and Y. D. Jiang, "Study on rock mechanics in deep mining engineering," *Chinese Journal of Rock Mechanics and Engineering*, vol. 24, no. 16, pp. 2803–2813, 2005.

[3] S. N. Dong, "Some key scientific problems on water hazards frequently happened in China's coal mines," *Journal of China Coal Society*, vol. 35, no. 1, pp. 66–71, 2010.

[4] S. X. Yin, W. J. Wu, Y. J. Li, G. L. Liu, and W. M. Yang, *Water Inrush in Karst Collapse Columns in North China Coalfields*, China Coal Industry Publishing House, Beijing, China, 2008.

[5] G. L. Liu, S. X. Yin, and Y. B. Wang, "Shear failure water inrush m ode at Karst sink hole bottom in North China coal field," *Coal Science and Technology*, vol. 35, no. 2, pp. 87–89, 2007.

[6] G. L. Liu, S. X. Yin, and Y. B. Wang, "Model of water inrush for thick wall cylinder at side face of paleo-sinkholes in North-China-type coalfields," *Journal of Engineering Geology*, vol. 15, no. 2, pp. 284–287, 2007.

[7] J. H. Tang, H. B. Bai, B. H. Yao, and Y. Wu, "Theoretical analysis on water-inrush mechanism of concealed collapse pillars in floor," *Mining Science and Technology (China)*, vol. 21, no. 1, pp. 57–60, 2011.

[8] Y. Q. Song, X. Y. Wang, P. Cheng, C. J. Peng, and S. Xu, "The mechanical criterion and numerical simulation of thick-walled elliptical cylinder collapse column model under water inrush," *Journal of China Coal Society*, vol. 36, no. 3, pp. 452–455, 2011.

[9] J. P. Xu, Y. Song, Y. H. Cheng, and Z. Q. Qiu, "Distributing of ground stress in and around Karst collapse column," *Journal of Mining & Safety Engineering*, vol. 22, no. 4, pp. 118–120, 2005.

[10] J. C. Wang and J. B. Li, "Physical model and theoretic criterion of the forecast of water inrush caused by collapse columns," *Journal of University of Science and Technology Beijing*, vol. 32, no. 10, pp. 1243–1247, 2010.

[11] J. C. Wang, J. B. Li, and G. M. Xu, "Development and application of simulation test system for water inrush from the water-conducting collapse column," *Journal of Mining Safety Engineering*, vol. 27, no. 3, pp. 305–309, 2010.

[12] W. Q. Liu, *Studies on Seepage Theory in Over-Broken Rock Mass and its Application*, China University of Mining & Technology, Xuzhou, China, 2002.

[13] X. X. Miao, W. Q. Liu, and Z. Q. Chen, *Seepage Theory of Mining Rock Mass*, The Science Publishing Company, Beijing, China, 2004.

[14] X. X. Miao, S. C. Li, and Z. Q. Chen, "Bifurcation and catastrophe of seepage flow system in broken rock," *Mining Science and Technology (China)*, vol. 19, no. 1, pp. 1–7, 2009.

[15] Z. G. Ma, X. X. Miao, X. H. Li, G. L. Guo, and X. S. Shi, "Permeability of broken shale," *Journal of Mining Safety Engineering*, vol. 24, no. 3, pp. 260–264, 2007.

[16] Z. G. Ma, X. X. Miao, F. Zhang, and Y. S. Li, "Experimental study into permeability of broken mudstone," *Journal of China University of Mining Technology*, vol. 17, no. 2, pp. 147–151, 2007.

[17] Z. G. Ma, G. L. Guo, R. H. Chen, and X. B. Mao, "An experimental study on the compaction of water-saturated over-broken rock," *Chinese Journal of Rock Mechanics and Engineering*, vol. 24, no. 7, pp. 1139–1144, 2005.

[18] M. G. Sun, T. Z. Li, X. W. Huang, and R. H. Chen, "Penetrating properties of non-Darcy flow in fragmentized rocks," *Journal of Anhui University of Science and Technology (Natural Science)*, vol. 23, no. 2, pp. 11–13, 2003.

[19] W. K. Bu, "Experimental study of permeability of broken rock sampled from strata containing faults," *Journal of Experimental Mechanics*, vol. 27, no. 4, pp. 469–473, 2012.

[20] C. Z. Du, W. Q. Liu, Y. L. He, and H. L. Zhao, "Experimental study of non-steady laws on over-broken rock seepage with compaction," *Ground Pressure and Strata Control*, vol. 21, no. 1, pp. 109–111, 2004.

[21] X. X. Miao, S. C. Li, and Z. Q. Chen, "Experimental study of seepage properties of broken sandstone under different porosities," *Transport in Porous Media*, vol. 86, no. 3, pp. 805–814, 2010.

[22] D. Ma, X. X. Miao, Y. Wu et al., "Seepage properties of crushed coal particles," *Journal of Petroleum Science and Engineering*, vol. 146, pp. 297–307, 2016.
[23] D. Ma, H. B. Bai, Z. Q. Chen, and H. Pu, "Effect of particle mixture on seepage properties of crushed mudstones," *Transport in Porous Media*, vol. 108, no. 2, pp. 257–277, 2015.
[24] S. C. Li, *Nonlinear Dynamic Study on Non-Darcy Flow in Broken Rock Mass*, China University of Mining Technology, Xuzhou, China, 2006.
[25] T. Z. Li, L. Ma, and L. Y. Zhang, "Discussion about positive or negative sign of permeability indexes in non-Darcy flow of mudstone," *Journal of Mining Safety Engineering*, vol. 24, no. 4, pp. 481–485, 2007.
[26] Z. Q. Chen, S. C. Li, H. Pu, and X. W. Huang, *Coupling Dynamics of Creep and Seepage of Mining Rock*, The Science Publishing Company, Beijing, China, 2010.
[27] B. H. Yao, *Research on Variable Mass Fluid-Solid Coupling Dynamic Theory of Broken Rock Mass Application*, China University of Mining & Technology, Xuzhou, China, 2012.
[28] D. Ma, *Experimental Research on Non-Darcy Flow Seepage Properties of Broken Mudstone with Variable Mass*, China University of Mining & Technology, Xuzhou, China, 2013.
[29] L. Z. Wang, *Accelerated Experimental Study on Permeability for Broken Mudstone with Mass Loss*, China University of Mining Technology, Xuzhou, China, 2014.
[30] L. Z. Wang, H. L. Kong, Z. Q. Chen et al., "A sustainable pressurized osmosis device for seepage test of rock mass," China Patent 201410031033.2, 2014.
[31] L. Z. Wang, H. L. Kong, Z. Q. Chen, B. Y. Yu, Y. Han, and Z. F. Wang, "A compatible penetration test device for syringe type and pump station," China Patent 201520827913.0, 2015.
[32] L. Z. Wang, Z. Q. Chen, and H. L. Kong, "An experimental investigation for seepage-induced instability of confined broken mudstones with consideration of mass loss," *Geofluids*, vol. 2017, Article ID 3057910, 12 pages, 2017.
[33] L. Z. Wang and H. L. Kong, *Accelerated Experimental Study on Permeability for Broken Rock Accompanying with Mass Loss*, The Science Publishing Company, Beijing, China, 2017.
[34] L. Z. Wang and H. L. Kong, "Variation characteristics of mass-loss rate in dynamic seepage system of the broken rocks," *Geofluids*, vol. 2018, Article ID 7137601, 17 pages, 2018
.